ACS APPLIED MATERIALS & INTERFACES

Research Article

www.acsami.org

Convenient Fabrication of Electrospun Prolamin Protein Delivery System with Three-Dimensional Shapeability and Resistance to Fouling

Yixiang Wang, Jingqi Yang, and Lingyun Chen*

Department of Agricultural, Food, and Nutritional Science, University of Alberta, Edmonton, Alberta, Canada T6G 2P5

ABSTRACT: It has been newly discovered that by simply altering the applied voltage, the resultant electrospun prolamin protein fabrics can rapidly (within 30 s) form either flat sheets or self-rolled tubes when immersed in water. This phenomenon opens up many potential biomedical applications for drug delivery. The morphology and structure of both dry and wet fibers were characterized in detail. The hordein/zein fibers fabricated at relatively lower voltage were stabilized by the preaggregated nanoscale hydrophobic domains and exhibited restricted swelling while maintaining a flat sheet shape with minimal changes to secondary structure when immersed in water. By applying a higher voltage, we triggered a greater bending instability during the electrospinning process, and the hordein/zein network structure generated could rapidly relax in an aqueous environment. This increased mobility of molecular chains allowed the uneven aggregation of hydrophobic dopants, which catalyzed the self-rolling of the aligned fibers. Sessile drop measurements even showed a reduction in the contact angle from 106 to 39° for the fibers with 50% zein prepared at raised voltage, indicating the conversion of surface properties caused by the relaxation. All the fibers demonstrated low toxicity in human primary dermal fibroblast cell culture. Moreover, the electrospun fabrics exhibited a strong resistance to protein adsorption and cell attachment, and the release experiment indicated that both three-dimensional porous structures could serve as a carrier for controlled release of incorporated bioactive compounds into phosphate-buffered saline. Therefore, these electrospun prolamin protein fabrics represent an ideal and novel platform to develop nonadherent drug delivery systems for wound dressing and other biomedical applications.

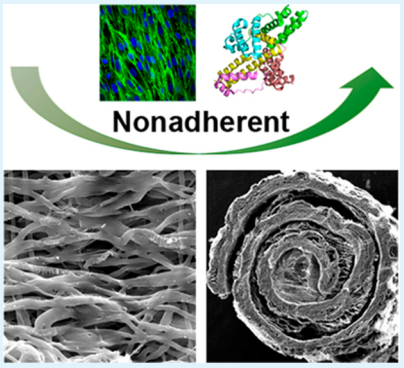

KEYWORDS: *prolamin proteins, electrospun fibers, delivery system, three-dimensional shapeability, antifouling*

1. INTRODUCTION

The fabrication of various microstructures for specific applications relating to three-dimensional (3D) vehicles for drug delivery is a rapidly growing area of research.[1] Attention has been paid to the development of appropriate fabrication machinery that allows 3D drug delivery systems (DDS) to be produced in a simple, reliable, and reproducible manner.[2] A number of manufacturing processes have been explored to form 3D DDSs, such as electrospinning, wet spinning, melt extrusion, and 3D printing. Among these techniques, electrospinning has been widely accepted as the simplest and least expensive means to make ultrafine fibers composed of 3D network.[3] The most particular advantages of electrospun submicron/nano fabrics are their very large surface area to volume ratio and excellent pore-interconnectivity. These attributes allow quickly starting signaling pathways and facilitating the transportation of bioactive compounds.[4] A wide variety of both natural and synthetic polymers has been applied to make electrospun DDSs. However, the poor shapeability of electrospinning limits its use in biomedical applications where different shapes and dimensions of materials are required.[5] For example, in order to form a tubular scaffold, a thin rotating mandrel with the diameter of 4−6 mm must be employed as the collector. These fibers are deposited on a limited area, which results in a low production efficiency.[6−8] Alternatively, the electrospun fabrics gathered by a plate collector have to be manually rolled up and secured by using glue.[3,9,10] To the best of our knowledge, an electrospun 3D DDS system with self-shapeability has been seldom reported.

The resistance to protein and cellular fouling is important for DDSs applied in the biomedical field. The release of drugs from DDSs can be interrupted by nonspecific adsorption of biomolecules on the scaffold surface and the adherence of wound dressings may cause severe pain and bleeding upon removal of the dressing.[11] The hydrophobic/hydrophilic nature of a substrate is a critical factor when engineering the surface properties in various biomedical applications because hydrophilic membrane surfaces are less prone to the microbial adhesion that initiates biofouling.[12] For example, in the separation of protein solutions, hydrophilic membranes are favorable due to the minimized protein adsorption. Similarly, hydrophilic scaffolds are preferred for some tissue-engineering applications and wound dressings,[13] whereas hydrophilic electrospun fabrics usually lose their overall shape or readily dissolve in water. Most of the synthetic polymer fibers are either hydrophobic or slightly hydrophilic, which cannot

Received: March 11, 2015
Accepted: June 1, 2015
Published: June 1, 2015

DOI: 10.1021/acsami.5b02129
ACS Appl. Mater. Interfaces 2015, 7, 13422−13430

effectively resist nonspecific protein adsorption and prevent cell attachment.[14] To obtain a hydrophilic surface, researchers have investigated several approaches for surface modification of membranes, such as surface grafting polymerization, coating, and blending.[15,16] Many different surface preparations based on polyethylene glycol (PEG) have been developed to prevent fouling, in which PEG is immobilized on surfaces. Nevertheless, this technique is limited by low polymer densities and relatively thin coatings.[17] Recently, there has been considerable interest in developing new antifouling membranes, especially ones based on renewable resources.

Zein and hordein are the major storage proteins from corn and barley, respectively, and are largely available as the byproducts of starch or beta-glucan processing. To develop improved utilization of these coproducts from the industrial processing of cereal crops, we employed them as raw materials to fabricate electrospun DDSs in our previous work.[18−20] Currently, a novel self-shapeability of electrospun hordein/zein fabrics was observed when the samples were prepared at a higher applied voltage rather than the "normal" value. Different 3D shapes, namely flat sheets and self-rolled tubes, could rapidly form once the fabrics made at different voltages were immersed in water. These structural and conformational changes of electrospun prolamin protein fibers were investigated for the first time to explain their shapeable behaviors. In addition, the surface properties of prolamin protein fibers were demonstrated, and their controlled release profile was evaluated in simulated human body fluid.

2. EXPERIMENTAL METHODS

2.1. Materials. Zein (F4000, protein content of 92%, approximate molecular weight of 35,000, and total ash of 2% maximum) was purchased from Freeman Industries LLC (New York) and used without further purification. Regular barley grains (Falcon) were kindly provided by Dr. James Helm, Alberta Agricultural and Rural Development, Lacombe, Alberta. Barley protein content was 13.2 wt % (dry status), as determined by combustion with a nitrogen analyzer (FP-428, Leco Corporation, St. Joseph, MI) calibrated with analytical reagent grade EDTA (a factor of 6.25 was used to convert the nitrogen to protein). Hordein (total ash of 2% maximum) was extracted using the alcohol method according to our previous work, and the protein content (dry status) was 92 wt %, as determined by the same nitrogen analyzer.[21] Fluorescein isothiocyanate (FITC), bovine serum albumin (BSA, Fraction V), and riboflavin were purchased from Sigma-Aldrich Canada Ltd. (Oakville, ON, Canada). The normal adult human primary dermal fibroblasts cell line (ATCC PCS-201-012) was obtained from the American Type Culture Collection (Rockville, MD). Acetic acid and all other chemical reagents were purchased from Fisher Scientific (Markham, ON, Canada) and were used as received unless otherwise described.

2.2. Aligned Electrospun Hordein/Zein Fibers. The sample components and electrospinning conditions are listed in Table 1. Desired amounts of hordein and zein were blended in a mortar, and then dispersed in 3 mL pure acetic acid. The solutions were allowed to stir at room temperature for 4 h. Aligned hordein/zein ultrafine fibers were subsequently fabricated by a customized digital Electrospinning Apparatus EC-DIG (IME Technologies, Eindhoven, Netherlands) at room temperature. The above prepared solutions were forced through a blunt needle with a diameter of 0.8 mm at the rate of 1.6 mL h^{-1}, and the applied voltage was fixed at 15 or 25 kV. A rotating drum with a diameter of 10 cm was chosen as the collector, and the distance between the tip and collector was set at 15 cm. A rotating speed of 2000 rpm was used to prepare uniaxially aligned electrospun fibers. The obtained fabrics with the thickness of 0.08 mm were coded as hz30−15, hz30−25, hz50−15 and hz50−25, corresponding to a zein content (based on the total protein content) of 30 and 50 wt % and an applied voltage of 15 and 25 kV, respectively. The total hordein/zein content in each sample was constant.

Table 1. Various Components of Hordein/Zein Solutions and Electrospinning Conditions

	solution components					
sample	hordein (g)	zein (g)	acetic acid (mL)	potential (kV)	distance (cm)	Flow rate (mL/h)
hz30−15	0.38	0.16	3	15	15	1.60
hz30−25	0.38	0.16		25		
hz50−15	0.27	0.27		15		
hz50−25	0.27	0.27		25		

2.3. Fiber Morphology. Morphology observations of electrospun fibers were carried out with a Philips XL-30 scanning electron microscope (SEM) at an acceleration voltage of 5−10 kV. The samples were vacuum-dried for 24 h and then removed from the fabric with the support of aluminum foil. They were sputtered with gold for 2 min prior to observation and photographing. The morphology of electrospun fibers at wet status was recorded by immersing the fibers in water bath for 24 h at 20 °C. The resultant samples were frozen in liquid nitrogen and freeze-dried for SEM observation. In the SEM photos, fiber diameters were determined with the ImageJ image-visualization software developed by the National Institute of Health.[22] Two hundred random positions were selected and measured for each sample.

2.4. Structures of Electrospun Fibers. FTIR spectra of electrospun fibers were recorded on a Nicolet 6700 spectrophotometer (Thermo Fisher Scientific Inc., Waltham, MA). The samples were vacuum-dried for 24 h and then placed on an attenuated total reflectance (ATR) accessory equipped with a Ge crystal. The fibers immersed in a water bath for 24 h at room temperature were frozen in liquid nitrogen and freeze-dried before testing. Spectra were recorded as the average of 256 scans at 2 cm^{-1} resolution and 25 °C, using the empty accessory as blank. During measurements the accessory compartment was flushed with dry nitrogen. ATR correction, Fourier deconvolution and quantitative secondary structure analysis were performed using the software provided with the spectrometer (Omnic 8.1 software). Fourier self-deconvolution was applied in order to narrow finer bands hidden in larger bands. Parameters used for deconvolution with an enhancement of 2 and bandwidth of 20 cm^{-1}.

TEM observation (JEM-2200, JEOL TEM, Japan) of electrospun fibers was carried out to evaluate the phase separation in hordein/zein composites. The fibers were embedded in Spurr resin and cured at 70 °C overnight. They were trimmed with a razor blade and then with an ultracut microtome equipped with a glass knife, to obtain an extremely smooth trapezoidal cross-sectional surface. An ULTRACUT E microtome was used for ultrathin microtome. The top layer (about 1 mm) was first removed using a glass knife, then ultrathin sections of about 100 nm thickness were cut with a diamond knife at room temperature. The sections were mounted on 300 mesh Cu/Pd grids and stained by OsO_4 vapor for 18 h. They were finally examined on TEM operating at an accelerating voltage of 80 kV.

2.5. Contact Angle Measurement. The water contact angles of electrospun fibers were characterized by a contact angle goniometer (KRUSS DSA 10, Germany) using the sessile drop method. A piece (2 × 2 cm) of sample was fixed on a microscope slide by double-faced adhesive tape to prevent the rolling of the flat surface during wetting. Water droplets (2 μL) were then placed on the sample surfaces. Images were captured and analyzed with the goniometer at room temperature. The contact angle was measured and given by the goniometer based on the shape of the sessile drop, and the measurement was repeated for at least three samples of the same material with three tests for each sample.

DOI: 10.1021/acsami.5b02129
ACS Appl. Mater. Interfaces 2015, 7, 13422−13430

Table 2. Diameters of Aligned Electrospun Hordein/Zein Fibers, Dry and Immersed in Water for 24 h

	dry					immersed in water for 24 h				
sample	m (μm)	s^2	d_n (μm)	d_l (μm)	P_d	m (μm)	s^2	d_n (μm)	d_l (μm)	P_d
hz30−15	0.97	0.04	0.98 ± 0.23	1.04	1.06	1.61	0.03	1.61 ± 0.32	1.67	1.04
hz30−25	0.68	0.37	0.65 ± 0.29	0.78	1.20	1.60	0.02	1.78 ± 0.38	1.86	1.04
hz50−15	0.95	0.04	1.02 ± 0.27	1.10	1.08	1.31	0.06	1.36 ± 0.31	1.43	1.05
hz50−25	0.64	0.03	0.64 ± 0.18	0.69	1.08	1.23	0.08	1.21 ± 0.34	1.31	1.08

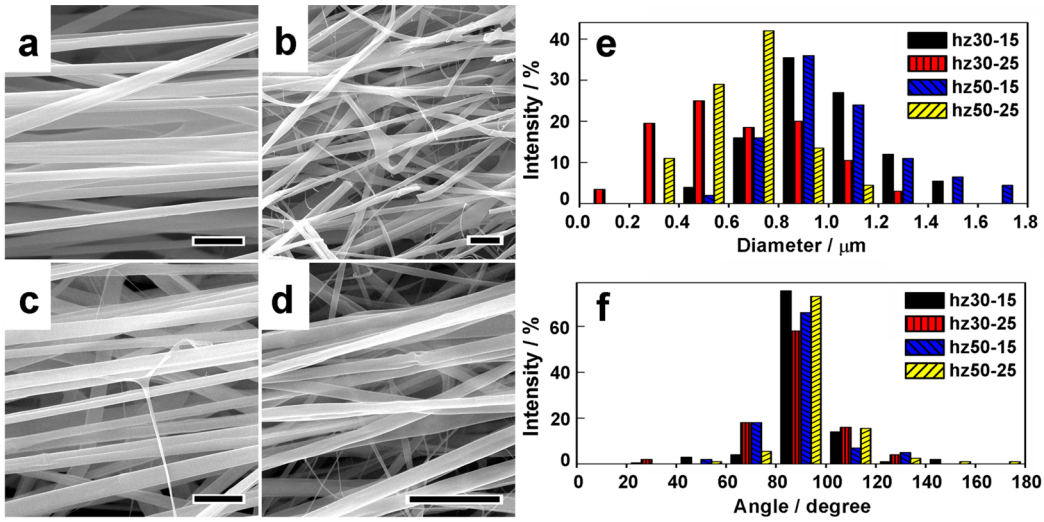

Figure 1. SEM images of orientated electrospun hordein/zein fibers at dry status: (a) hz30−15, (b) hz30−25, (c) hz50−15, and (d) hz50−25. Scale bar: 5 μm. (e) Diameter and (f) angle distributions of orientated electrospun hordein/zein fibers.

2.6. Protein Adsorption. Protein adsorption was tested as described by Grafahrend et al.[13] Briefly, three pieces (1 × 1 cm) of electrospun fibers were taken from each sample and incubated for 20 min in a 50 μg/mL solution of FITC labeled BSA in PBS buffer. Afterward, the samples were incubated three times for 20 min and another time for 60 min in PBS buffer. All samples were kept in the dark during the incubation steps and then observed with a CLSM 510 Meta confocal laser scanning microscope (Carl Zeiss, Jena, Germany). An oil immersion objective (40×) was used to visualize the samples, and images were processed with ZEN 2011 LE software.

2.7. Cell Attachment and in Vitro Cytotoxicity Assay. The electrospun fabrics with 1 mm thickness were soaked in water for 24 h, sterilized under UV radiation for 2 h, and thoroughly rinsed with copious amount of sterile PBS. Normal adult human primary dermal fibroblasts (5×10^4 cells per device) were seeded onto each sample and allowed to incubate for 48 h at 37 °C in 5% CO_2. Subsequently, the cells were fixed with an ice-cold solution of 3.7% formaldehyde in PBS (0.01 M, pH 7.4) for 30 min, and washed three times with PBS. The cell nuclei were then stained with DAPI (1 μg/mL in PBS), and the cell membranes were stained with Alexa Fluor 488 conjugate (5 μg/mL in PBS). The fluorescence images were taken on the CLSM 510 Meta confocal laser scanning microscope. The morphology of the freeze-dried electrospun fabrics with attached cells was also observed by SEM.

In vitro cytotoxicity was evaluated by MTT assay. Control experiment was carried out using only complete growth culture medium. The human dermal fibroblasts at a density of 5.0×10^3 cells per well were seeded in the 96-well plate with or without the presence of prolamin fabrics. After incubation for 48 h in incubator (37 °C, 5% CO_2), 100 μL MTT solution was added to each well. After 4 h incubation at 37 °C, 100 μL dimethyl sulfoxide was added to dissolve the formazan crystals. The dissolvable solution became homogeneous after about 15 min of shaking, and then was transferred into another 96-well plate. The optical density (OD) was measured at 570 nm with a Microplate Reader Model 550 (BIO-RAD, Hercules, CA). The cell viable rate was calculated by the following equation:[23]

$$\text{viable cells (\%)} = \text{OD}_{\text{treated}}/\text{OD}_{\text{control}} \times 100 \quad (1)$$

where $\text{OD}_{\text{treated}}$ and $\text{OD}_{\text{control}}$ were obtained in the presence or absence of prolamin fabrics, respectively.

2.8. Controlled Release. Riboflavin was selected as a bioactive molecule model to investigate the release properties of electrospun hordein/zein fibers. Drug-loaded fibers were prepared by dispersing riboflavin in hordein/zein solutions before electrospinning and the riboflavin content was 5 wt % in the final electrospun fibers. The release kinetics was assessed in phosphate-buffered saline (PBS, pH 7.4) with a 2100C dissolution system (Distek, Inc., Brunswick Township, NJ). Riboflavin-loaded fibers (40 mg) were placed into 50 mL PBS at 37 °C and stirred at 100 rpm. The riboflavin content in the release mediums was monitored with S-3100 UV−vis spectrophotometer (Scinco Co., Ltd., Japan) at a wavelength of 445 nm.

2.9. Statistical Analysis. Experimental results were represented as the mean of five batches ± SD. Statistical evaluation was carried out by analysis of variance (ANOVA) followed by multiple-comparison tests using Duncan's multiple-range test at the 95% confidence level. All of the analyses were conducted using SAS statistical software (SAS Institute, Inc., Cary, NC) with a probability of $p < 0.05$ considered to be significant.

3. RESULTS AND DISCUSSION

3.1. Three-Dimensional Shapeability of Electrospun Fibers. Electrospun hordein/zein fibers were prepared at two hordein-to-zein ratios of 70:30 and 50:50 and under two voltages of 15 and 25 kV. According to our previous work,[19] the hz30 and hz50 fibers were selected due to their good mechanical properties and stability. Two applied voltages were chosen in this work, where 15 kV was the optimized value for prolamin protein to form regular fine fibers, and 25 kV was employed as the high voltage condition. Fiber morphology at dry and wet status was observed by SEM, and the fiber diameter and angle distributions were determined with the

DOI: 10.1021/acsami.5b02129
ACS Appl. Mater. Interfaces 2015, 7, 13422−13430

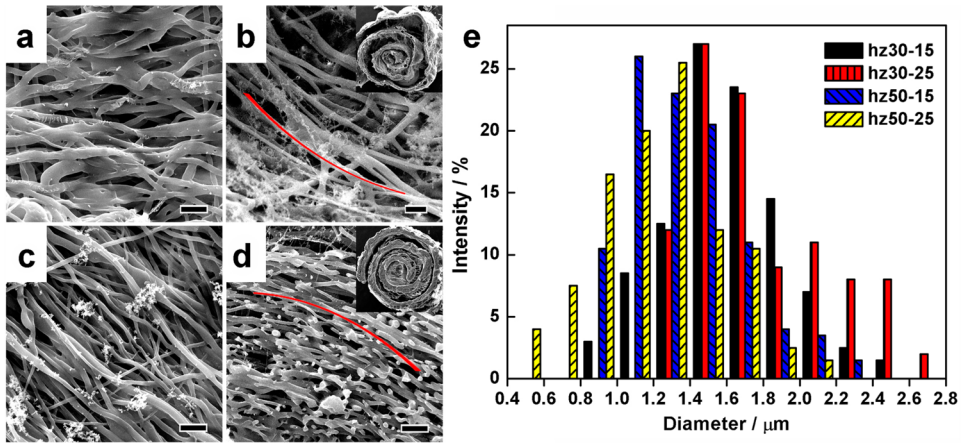

Figure 2. SEM images and diameter distribution of orientated electrospun hordein/zein fibers after immersing in water for 24 h: (a) hz30−15, (b) hz30−25, (c) hz50−15, and (d) hz50−25. Scale bar: 5 μm. (e) Diameter distribution.

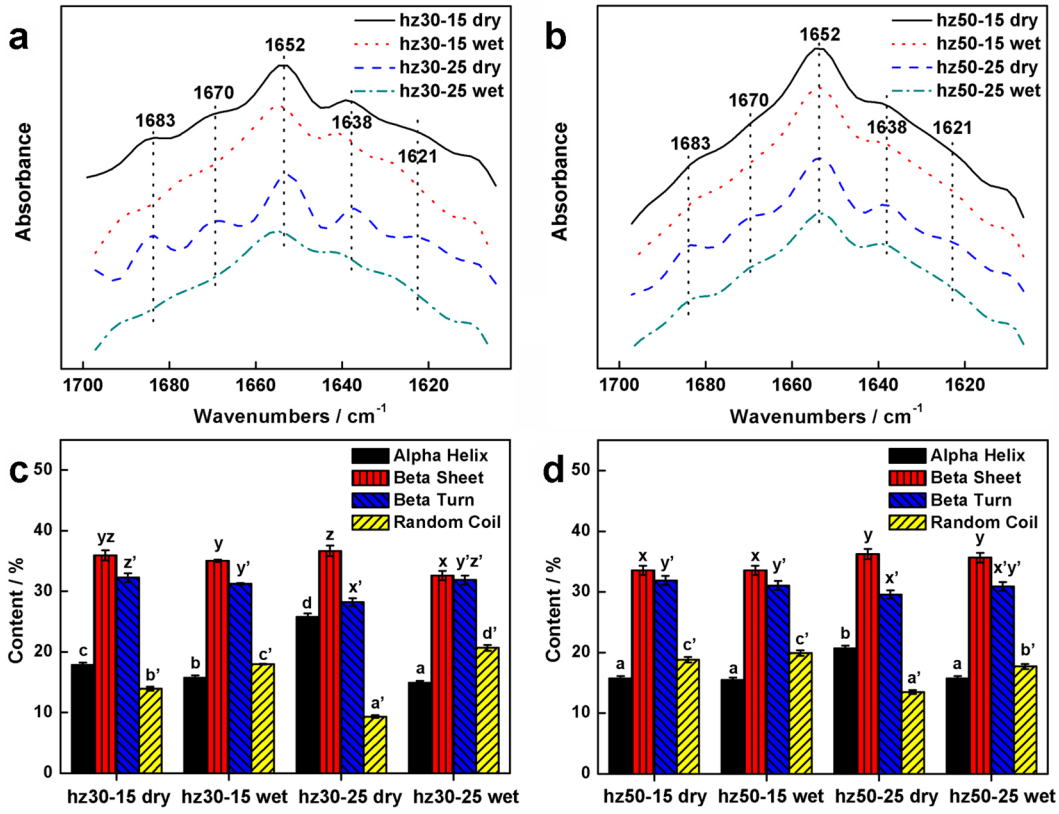

Figure 3. (a and b) Fourier-deconvoluted FTIR spectra and (c and d) secondary structure content of orientated electrospun hordein/zein fibers. Different groups of letters (abcd, xyz, x′y′z′ and a′b′c′d′) on the top of the columns indicate the significant difference ($p < 0.05$) of the content of α helix, β sheet, beta turn, and random coil due to applied voltage and water treatment.

ImageJ image-visualization software by measuring two hundred random positions for each sample. Log-normal function D was used to describe the size-distribution of the fibers:[24]

$$D = A \exp[-(\ln(x) - \ln(m))^2/s^2] \quad (2)$$

where m is the mode and s^2 is the variance. All diameter distributions were properly fitted, and the parameters m and s^2 are listed in Table 2. Number-average diameters (d_n) and diameter-weighted average values (d_l) were calculated as well. The diameter polydispersity index was therefore defined as $P_d = d_l/d_n$. As shown in Figure 1a,c, the hz30−15 and hz50−15 fibers exhibited a smooth surface and uniform size (s^2 value of 0.04 and P_d values of 1.06−1.08), suggesting a good electrospinnability of hordein/zein solutions at the voltage of 15 kV. In acetic acid, hordein molecules were unfolded and reorganized to form an extended and flexible conformation. Strong interactions thus existed among hordein molecules and led to the narrow electrospinnable conditions of hordein solution.[18] Zein particles were added to the system as the plasticizer to decrease the strong interactions among hordein molecules and improve the electrospinnability. When the applied voltage increased to 25 kV, a wide diameter distribution (large s^2 value of 0.37 and P_d value of 1.20) was observed for hz30−25 fibers, which indicates an unstable electrospinning

DOI: 10.1021/acsami.5b02129
ACS Appl. Mater. Interfaces 2015, 7, 13422−13430

process. However, the hz50−25 fibers showed narrow diameter distribution again with s^2 and P_d values similar to those prepared at 15 kV. The diameter of electrospun hordein/zein fibers significantly decreased from 0.98 ± 0.23 and 1.02 ± 0.27 μm to 0.65 ± 0.29 and 0.64 ± 0.18 μm, respectively, when the fibers were prepared at 25 kV. The solutions may have been ejected and the prolamin protein molecules were stretched and orientated by the strong Coulombic force during the electrospinning process. The higher the applied voltage was, the more the fibers were stretched. Therefore, extra zein particles (50 wt %) were required as plasticizer to overcome the strong interactions among hordein molecules during electrospinning at higher voltage, leading to the stable process and uniform fiber size. Figure 1f shows the angle distribution of electrospun hordein/zein fibers. To clearly display the alignment degree of different samples, we defined the orientation of most fibers in each sample as 90°. All of them had a restricted angle distribution, which revealed that the fibers, despite of their preparation conditions, were successfully aligned on the rotating drum collector.

The SEM images and diameter distribution of aligned electrospun hordein/zein fibers after immersed in water for 24 h are shown in Figure 2. Different from the neat hordein and zein fibers, which suffered for their poor stability and limited application in an aqueous environment,[19] all the samples preserved the fiber shape in water. A certain extent of swelling was observed, but these electrospun fabrics still exhibited a well-designed porous structure and thus enabled a large surface area to volume ratio and excellent pore-interconnectivity. Interestingly, hz30−25 and hz50−25 fibers self-rolled into tubular shape with the diameter of about 1.40 mm (Figure 2, b,d, insets), whereas hz30−15 and hz50−15 kept their sheet shape. These structures were well maintained even after immersion in water for 24 h. The self-assembled tubes from hz50−25 fibers showed a regular shape compared to those from hz30−25 fibers, which probably related to the wide size distribution of hz30−25 caused by the unstable electrospinning process. The swelling behavior of electrospun hordein/zein fibers was associated with the applied voltage. The swelling degree of hz30−15 and hz50−15 was 1.64 ± 0.50 and 1.33 ± 0.46, respectively, which were lower than that of cross-linked PVA/hyaluronic acid (HA) fibers.[25] Nevertheless, the swelling degree of hz30−25 and hz50−25 obviously increased to 2.74 ± 1.35 and 1.89 ± 0.75, respectively. These differences suggest that electrospinning voltage can be applied to modulate fiber molecular structures, which has also been proven in the electrospun poly(L-lactic acid)/poly(D-lactic acid)[26] and poly(p-phenylenevinylene)/poly(vinylpyrrolidone)[27] fibers. However, the voltage induced self-rolling of electrospun fabrics when immersed in water has never been reported.

3.2. Electrospun Fiber Structure. Protein conformation plays an important role in determining the properties of protein materials. Thus, FTIR was applied to study the protein conformational changes caused by different applied voltages and water. The Fourier self-deconvolution spectra within the amide I region (1600−1700 cm^{-1}) and the calculated secondary structure contents of electrospun hordein/zein fibers before and after immersion in water are shown in Figure 3. The dry hz30−15 fibers exhibited several bands, which have been assigned to protein secondary structures: 1683 cm^{-1} (β-sheet), 1670 cm^{-1} (β-turn), 1652 cm^{-1} (α-helix), 1638 cm^{-1} (β-sheet), and 1621 cm^{-1} (β-sheet).[28] The fibers prepared at 25 kV exhibited similar peaks, but the intensity of these peaks obviously increased. It indicated that more secondary structures were generated at higher voltage. At the same time, the content of α-helical structure substantially rose and the amount of random coils reduced. During the preparation of electrospun hordein/zein fibers, the major secondary structure of zein was well maintained, while the original structure of hordein was initially unfolded in acetic acid, and then stretched in the presence of a strong Coulombic force. This process promoted the formation of α-helical structures which could be ascribed to an electrically driven bending instability.[18,29] Therefore, a stronger bending instability was triggered when the applied voltage increased, leading to the addition of α-helical structure in hz30−25 and hz50−25. When the fibers were immersed in water, the protein secondary structure components in hz30−15 slightly changed, showing good stability. However, a significant loss of secondary structure was observed for hz30−25, as demonstrated by the decrease in both α-helix and β-sheet structures, and the increase in random coils. The similar changes occurred for the hz50−15 and hz50−25 fibers. Elastomers/rubbers have glass transition temperatures (T_g) lower than room temperature, so their chain segments are able to move (i.e., rearrange their conformations) in electrospun nanofibers, and the molecular movement/relaxation will occur when the stretching force no longer exists, particularly during the bending instability.[30] The T_g value of barley protein powder is 60.1 °C,[31] and thus, the relaxation of hordein molecules at room temperature was favorable to take place when the fabrics were immersed in water rather than at dry status due to the plasticization of water molecules. For hz30−25 and hz50−25, more secondary structure and α-helix content were generated by the stretching force, so more relaxation occurred when immersed in water. The solvent molecules could easily penetrate into the fibers and exhibited a higher degree of swelling.

The hz50−15 and hz50−25 fibers were selected to further investigate the change of molecular structure. TEM images of OsO_4 stained ultrathin sections of hz50−15 and hz50−25 before and after being immersed in water for 24 h are shown in Figure 4. To clearly reveal their inner structure, we cut the samples perpendicularly and horizontally to the fiber direction for comparison. Osmium is highly electropositive with an initial oxidation state of +8 and gives rise to strong electron scattering from electron donor ligands, so OsO_4 is extensively used to stain unsaturated structures.[32] OsO_4 reacts with a hydrophobic double bond more than a hydrophilic carboxyl group, and has been recently used to indicate the periodic phase separation in nanostructured polymer particles.[32,33] Nanoscale black spots were present in the section of dry hz50−15, as shown in Figure 4a, indicating the hydrophobic aggregated domains formed in prolamin protein networks. The size of the spots decreased radially from the center to the surface of the fiber. This reflected the uneven mobility of prolamin protein molecules in the core and skin, where reassembling in the outer layer was partially restricted due to faster evaporation of solvent residue. After immersion in water, the distribution and size of black spots was nearly unchanged. The preaggregated hydrophobic domains likely acted as nanosized fillers to strengthen the electrospun hordein/zein fibers.[20] The scattered hydrophobic fillers ensured the uniform and controlled variation of fiber network, which explains the low swelling degree and slightly changed protein structures of hz50−15. Therefore, the electrospun fabric maintained the same sheet shape in water. On the contrary, almost no clearly defined individual black

DOI: 10.1021/acsami.5b02129
ACS Appl. Mater. Interfaces 2015, 7, 13422−13430

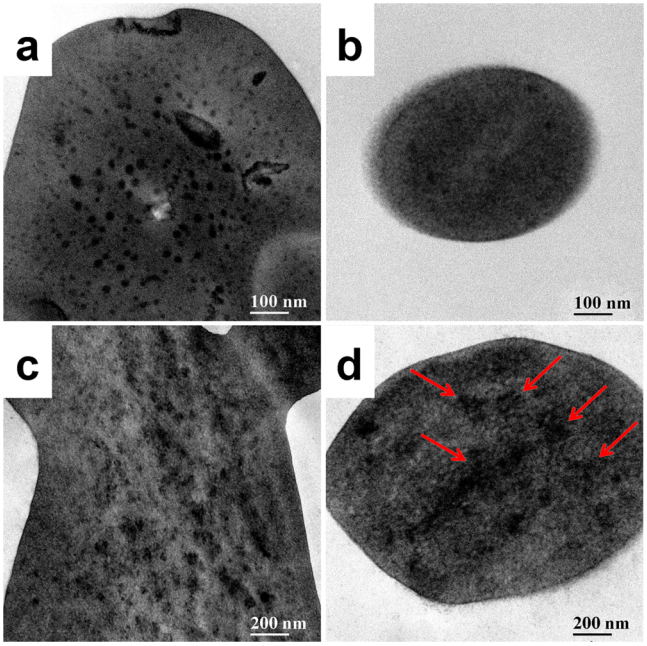

Figure 4. TEM images of OsO_4 stained ultrathin sections of (left) hz50−15 and (right) hz50−25: (a and b) dry status and (c and d) immersed in water for 24 h.

spots existed in the section of dry hz50−25, and the whole section was evenly stained, suggesting the homogeneous dispersion of hydrophobic dopants. The higher applied voltage may have triggered the formation of more organized structures as observed by FTIR, which restricted the reassembling of hydrophobic dopants, resulting in a restricted migration of fiber components at dry status. However, when the hz50−25 fibers were put in water, obvious swelling occurred and hydrophobic aggregated domains became visible again. As revealed by FTIR and SEM, the hordein molecules relaxed and the fiber network swelled in water, which provided the improved mobility of prolamin protein molecules and enabled the aggregation of hydrophobic dopants. This combined hydrophobic dopants formed unevenly distributed large aggregates inside the fiber, which caused a size mismatch and led to a buildup of internal stress, eventually generating the instability of fiber.[34] In our preliminary experiment, the hz50−25 fabric without orientation did not roll-up when immersed in water. This indicates the importance of the parallel piled up pattern of hz50−25 fibers for self-assembling into a tubular shape. Therefore, the bending of electrospun fibers was catalyzed by the formation of unevenly distributed hydrophobic aggregates (heterogeneity as shown in Figure 4d). Then the orientation of fibers could bend toward the same direction that was normal to the fabric surface, exhibiting the curled structure of electrospun fabric. This unique 3D shapeability provides a convenient way to fabricate structured devices such as self-assembled tubes for biological applications, controlled encapsulation, and release.[35]

3.3. Surface Property of Electrospun Fibers. Water-contact angles were measured for the electrospun hordein/zein fabrics so as to evaluate the surface wettability of the fibers prepared at different applied voltages. As shown in Figure 5a, hz30−15 exhibited a contact angle of 16.6 ± 0.9°, illustrating the high hydrophilicity of the fabrics. Compared to zein, which is solubile in 90% ethanol, hordein has a relatively weaker surface hydrophobicity with good solubility in 60% ethanol,

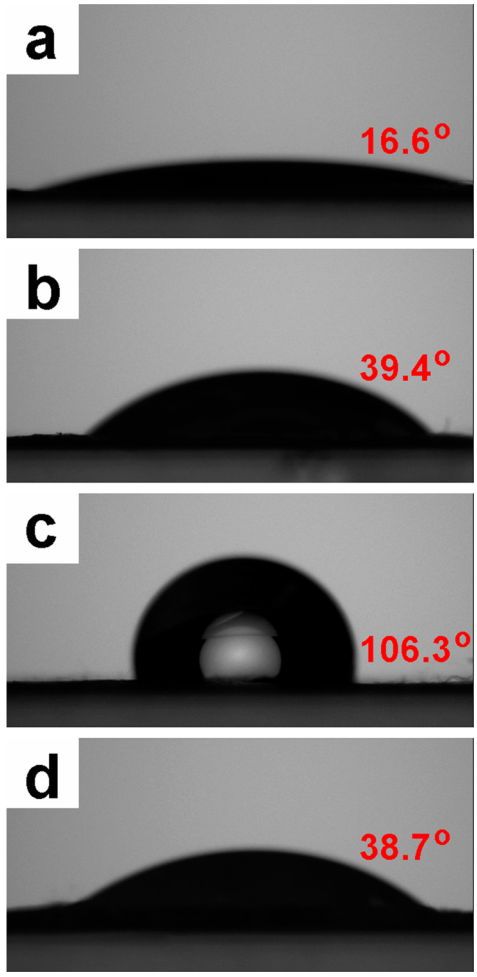

Figure 5. Images of contact angle measurements on orientated electrospun hordein/zein fibers: (a) hz30−15, (b) hz30−25, (c) hz50−15, and (d) hz50−25.

probably due to more exposed glutamic acid.[36] In the hz30−15 fibers, hordein molecules made up the matrix, so the fiber network was permeable to water and resulted in good wettability. The contact angle of hz30−25 slightly rose to 39.4 ± 0.8° because of the increased surface roughness triggered by the unstable electrospinning process.[37] It was not surprising that hz50−15 showed the high contact angle of 106.3 ± 1.9° because the continuity of hordein network was affected by the addition of more hydrophobic zein and the spread of water was restricted.[19] However, the contact angle of hz50−25 was only 38.7° ± 0.7, which was much smaller than that of the fibers fabricated at 15 kV with the same zein content. This means that the electrospun fiber surface property rapidly and largely changed during the water induced relaxation of hordein molecules. An entropy-driven movement of hydrophobic dopants toward the core of fiber occurred in order to reduce their surface area exposed to water.[38] These dopants lumped together and formed unevenly distributed aggregates inside the fiber, thus the hydrophilicity of the electrospun fabric surface increased.

3.4. Antifouling Properties of Electrospun Fibers. Figure 6 shows confocal microscopic images of electrospun hordein/zein fabrics incubated with FITC-labeled bovine serum albumin (BSA). No adsorbed BSA was found on hz30−15, hz30−25, and hz50−25, but hz50−15 exhibited a light green

DOI: 10.1021/acsami.5b02129
ACS Appl. Mater. Interfaces 2015, 7, 13422−13430

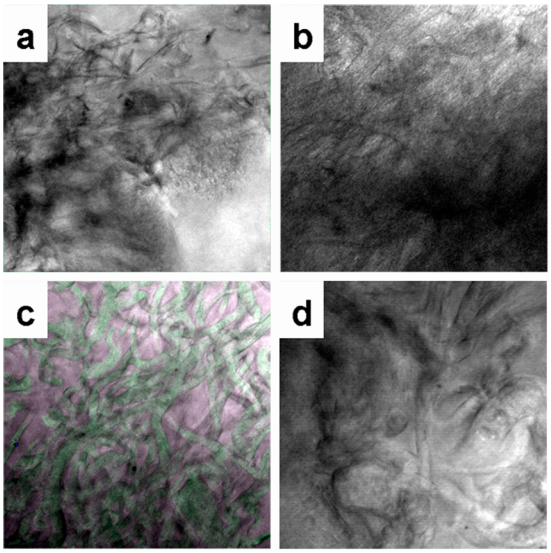

Figure 6. Confocal microscopic images of orientated electrospun hordein/zein fibers incubated with FITC-labeled bovine serum albumin: (a) hz30−15, (b) hz30−25, (c) hz50−15, and (d) hz50−25.

color. It revealed that the various hydrophobic/hydrophilic natures of the fibers determined the protein adhesive behavior, where the hydrophilic-enriched surfaces efficiently decreased BSA adsorption.

To explore the ability of electrospun hordein/zein fibers to resist cell attachment, we observed the growth and proliferation of normal adult human primary dermal fibroblasts on these protein fabrics by confocal microscope and SEM. Fibroblasts were chosen as a model due to their strong tendency to adhere on most substrates and their important role during wound healing and integration of biomaterials.[39] The cells were directly seeded onto the electrospun fabrics and allowed to incubate for 48 h. All the surfaces of prolamin protein fibers were found to be entirely resistant to cell attachment (only hz50−15 is shown in Figure 7b,c). Although the presence of a continuous phase of zein in hz50−15 led to the increased hydrophobicity and slight protein adsorption, the surface of hz50−15 could still prevent the cell attachment. Interestingly, an intact cell layer was formed on the bottom of the tissue culture plate (Figure 7a), which was just under the electrospun fabric. This proves that the observed cellular resistance of the fibers was not because of a soluble toxic component of protein fibers. In our previous work, we reported the good biocompatibility of hordein/zein fibers with primary epidermal keratinocytes (NHEK) cells.[19] Here, the effect of fibers on the growth and proliferation of fibroblasts was further determined by MTT cytotoxicity assay. As shown in Figure 7d, the viability of fibroblasts was higher than 90% for all the samples, indicating good biocompatibility. Therefore, the hz30−15 and hz30−25 fibers exhibited a remarkable antifouling behavior due to their hordein matrix, and the surface of hz50−25 was dramatically improved by the increased voltage triggered strong stretching and the following water-induced relaxation. These novel nonadherent 3D materials could be advantageous for potential applications in wound healing because they would not affect the recovery of damaged tissue while achieving a nonstick removal.[40] Moreover, the antifouling property will open opportunities for applications as biocompatible drug carriers, biosensors, medical implants, tissue engineering, or filtration

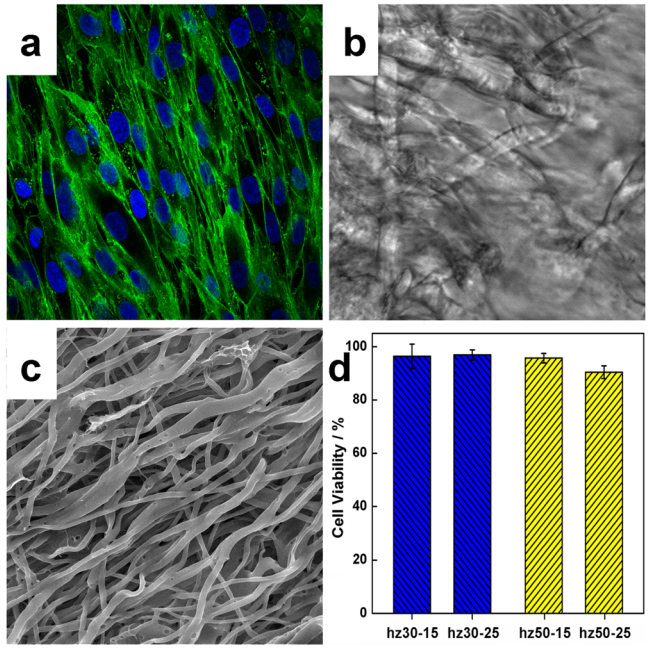

Figure 7. Confocal microscopic images of (a) fibroblast attachment on tissue culture plate and (b) the lack of attachment on hz50−15. (c) SEM image of hz50−15 with the lack of attachment. (d) Cytotoxicity of orientated electrospun hordein/zein fibers relative to the nontoxic control (growth culture medium) after incubation for 48 h.

systems because they will inhibit the adsorption of blood cells, fibroblasts, proteins, and possibly bacteria.[41]

3.5. Release Behavior of Electrospun Fibers. The release behavior of electrospun hordein/zein fibers prepared at different applied voltages was investigated in PBS at 37 °C to simulate a body fluid system (Figure 8). Riboflavin was

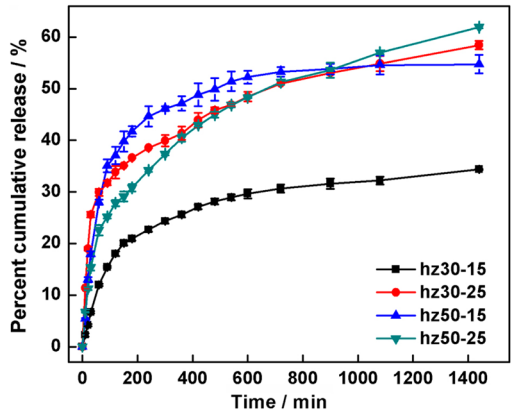

Figure 8. Release profiles of riboflavin from drug-loaded orientated electrospun hordein/zein fibers in PBS at 37 °C.

employed as a model bioactive molecule, and the resultant fabrics could still rapidly form the different 3D shapes, indicating that the incorporation of bioactive molecules (such as riboflavin) will not affect the self-shapeability of the delivery system. To reveal the effect of protein structure on the release behavior, we piled up several layers of fabrics for the dissolution test so as to prevent the self-rolling and dismiss the effect of 3D shapes. The Korsmeyer−Peppas semiempirical equation was applied to explore the mechanism of riboflavin release from electronspun fibers:[42]

DOI: 10.1021/acsami.5b02129
ACS Appl. Mater. Interfaces 2015, 7, 13422−13430

$$M_t/M_\infty = kt^n \quad (3)$$

where M_t/M_∞ is the fraction of model molecule released after time t relative to the amount of model molecule released at infinite time, k is a constant, and n is the diffusional exponent. Inferences about the release mechanism are based on the fit of this equation to the model molecule release data through 60% dissolution and comparison of the value of n to the semiempirical values for slab geometry reported by Peppas [$n \leq 0.50$ (Fickian diffusion), $0.50 < n < 1$ (anomalous transport) and $n = 1$ (case II transport)].[43] Riboflavin release from all the samples displayed a typical sigmoid profile with n values in the range of 0.66−0.81 (R^2 = 0.986−0.999) during the first 2 h and then 0.20−0.34 (R^2 = 0.988−0.995) in the remaining time. It indicated a two-stage release where enhanced riboflavin diffusion occurred at the beginning due to the water induced mobility of protein molecules. When the systems reached equilibrium, the release followed a diffusion-controlled mechanism. The hz30−15 fibers showed the slowest release rate and only 34.36% riboflavin was detected in the buffer after 24 h. This was due to the restricted swelling degree and the well-maintained 3D porous structure in PBS. The moderate release of riboflavin was observed for hz50−15. In hz50−15, the intensified phase separation affected the integrity of hordein network, which thus facilitated the diffusion within the fiber and led to the accelerated release in the first 2 h. With the increase of applied voltage, the hz30−25 fibers exhibited a rapid release in the first 30 min. This burst release phenomenon was related to the widest size distribution and highest swelling ratio of hz30−25 caused by the unstable electrospinning process. It was worth noting that the hz50−25 fibers displayed better control of this burst release. Only 27.83% riboflavin leached out after 2 h, which was much slower than those from hz50−15 and hz30−25. Considering the relatively high swelling degree of hz50−25, this reduced release in the first stage should be due to the migration of hydrophobic dopants toward the core of fibers and the formation of large aggregates during protein relaxation. There was an increased chance to build up the binding between riboflavin and hydrophobic dopants in this process, and some riboflavin molecules might be trapped in the aggregates to retard the burst release. The hz30−15 and hz50−25 fibers have the potential to be used as novel antifouling drug delivery systems with a controlled release behavior. Different from the traditional self-rolled solid bilayer polymer films, the electrospun prolamin protein fabrics exhibit excellent pore-interconnectivity and possess a large surface area to volume ratio. These features facilitate the transportation of the incorporated bioactive components, even when they were inserted in a limited space. Moreover, these biodegradable, biocompatible fabrics self-assemble when in water, making them suitable for encapsulation of sensitive compounds.[35]

4. CONCLUSION

For the first time, novel prolamin protein fabrics with controlled 3D shapeability were created with electrospinning. Particularly interesting, the self-rolling of electrospun fibers made at 25 kV occurred quickly when they were immersed in water, leading to the formation of tubular materials with a large surface area to volume ratio and excellent pore interconnectivity. These fibers exhibited a more ordered protein structure compared to those prepared at 15 kV, due to the stronger stretching generated by the Coulombic force during electrospinning. An obvious relaxation of prolamin protein molecules was then induced by water, which provided a chance for the hydrophobic dopants to migrate toward the core of fibers to form unevenly distributed large aggregates. This process built up an internal stress and caused instability, which catalyzed the bending and the eventual self-rolling of aligned electrospun fibers. It also resulted in an increased fiber surface hydrophilicity and an improved biomolecule release behavior. At the same time, the fibers fabricated at 15 kV were stabilized by their nanoscale hydrophobic domains. They showed a restricted degree of swelling and maintained a flat sheet shape even after immersing in water. This 3D shapeability suggests the potential to use these prolamin protein fabrics in various biomedical fields where either flat coatings or tubular inserts are needed. Overall, these fibers open the development of a novel nonadherent delivery systems, which possess excellent antifouling properties, low cell toxicity, and controlled release behaviors. Particularly, they may afford promising applications for healing of damaged tissues in the biomedical field.

AUTHOR INFORMATION

Corresponding Author

*Tel.: +1-780-492-0038; Fax: +1-780-492-8914. Email address: lingyun.chen@ualberta.ca (L. Chen).

Notes

The authors declare no competing financial interest.

ACKNOWLEDGMENTS

The authors are grateful to the Natural Sciences and Engineering Research Council of Canada (NSERC), Alberta Crop Industry Development Fund, Ltd. (ACIDF), Alberta Innovates Bio Solutions (AI Bio), and the Alberta Barley Commission for financial support, as well as Canada Foundation for Innovation (CFI) for equipment support. L.C. would like to thank the Natural Sciences and Engineering Research Council of Canada (NSERC)-Canada Research Chairs Program for its financial support.

REFERENCES

(1) Guo, S. Z.; Heuzey, M. C.; Therriault, D. Properties of Polylactide Inks for Solvent-Cast Printing of Three-Dimensional Freeform Microstructures. *Langmuir* **2014**, *30*, 1142−1150.

(2) Moulton, S. E.; Wallace, G. G. 3-Dimensional (3D) Fabricated Polymer Based Drug Delivery Systems. *J. Controlled Release* **2014**, *193*, 27−34.

(3) Shim, I. K.; Suh, W. H.; Lee, S. Y.; Lee, S. H.; Heo, S. J.; Lee, M. C.; Lee, S. J. Chitosan Nano-/Microfibrous Double-Layered Membrane with Rolled-up Three-Dimensional Structures for Chondrocyte Cultivation. *J. Biomed. Mater. Res., Part A* **2009**, *90*, 595−602.

(4) Lin, J.; Li, C.; Zhao, Y.; Hu, J.; Zhang, L. Co-electrospun Nanofibrous Membranes of Collagen and Zein for Wound Healing. *ACS Appl. Mater. Interfaces* **2012**, *4*, 1050−1057.

(5) Kim, M. S.; Kim, G. H. Highly Porous Electrospun 3D Polycaprolactone/β-TCP Biocomposites for Tissue Regeneration. *Mater. Lett.* **2014**, *120*, 246−250.

(6) Huang, C.; Wang, S.; Qiu, L.; Ke, Q.; Zhai, W.; Mo, X. Heparin Loading and Pre-endothelialization in Enhancing the Patency Rate of Electrospun Small-Diameter Vascular Grafts in a Canine Model. *ACS Appl. Mater. Interfaces* **2013**, *5*, 2220−2226.

(7) Marelli, B.; Alessandrino, A.; Farè, S.; Freddi, G.; Mantovani, D.; Tanzi, M. C. Compliant Electrospun Silk Fibroin Tubes for Small Vessel Bypass Grafting. *Acta Biomater.* **2010**, *6*, 4019−4026.

(8) Zhou, J.; Cao, C.; Ma, X. A Novel Three-Dimensional Tubular Scaffold Prepared from Silk Fibroin by Electrospinning. *Int. J. Biol. Macromol.* **2009**, *45*, 504−510.

DOI: 10.1021/acsami.5b02129
ACS Appl. Mater. Interfaces 2015, 7, 13422−13430

(9) Dinis, T. M.; Elia, R.; Vidal, G.; Dermigny, Q.; Denoeud, C.; Kaplan, D. L.; Egles, C.; Marin, F. 3D Multi-Channel Bi-functionalized Silk Electrospun Conduits for Peripheral Nerve Regeneration. *J. Mech. Behav. Biomed. Mater.* **2015**, *41*, 43−55.
(10) Kolambkar, Y. M.; Dupont, K. M.; Boerckel, J. D.; Huebsch, N.; Mooney, D. J.; Hutmacher, D. W.; Guldberg, R. E. An Alginate-Based Hybrid System for Growth Factor Delivery in the Functional Repair of Large Bone Defects. *Biomaterials* **2011**, *32*, 65−74.
(11) Kim, H. S.; Ham, H. O.; Son, Y. J.; Messersmith, P. B.; Yoo, H. S. Electrospun Catechol-Modified Poly(ethyleneglycol) Nanofibrous Mesh for Anti-fouling Properties. *J. Mater. Chem. B* **2013**, *1*, 3940−3949.
(12) Dasari, A.; Quirós, J.; Herrero, B.; Boltes, K.; García-Calvo, E.; Rosal, R. Antifouling Membranes Prepared by Electrospinning Polylactic Acid Containing Biocidal Nanoparticles. *J. Membr. Sci.* **2012**, *405*−*406*, 134−140.
(13) Grafahrend, D.; Calvet, J. L.; Klinkhammer, K.; Salber, J.; Dalton, P. D.; Möller, M.; Klee, D. Control of Protein Adsorption on Functionalized Electrospun Fibers. *Biotechnol. Bioeng.* **2008**, *101*, 609−621.
(14) Lalani, R.; Liu, L. Electrospun Zwitterionic Poly(sulfobetaine methacrylate) for Nonadherent, Superabsorbent, and Antimicrobial Wound Dressing Applications. *Biomacromolecules* **2012**, *13*, 1853−1863.
(15) Lee, J. W.; Jung, J.; Cho, Y. H.; Yadav, S. K.; Baek, K. Y.; Park, H. B.; Hong, S. M.; Koo, C. M. Fouling-Tolerant Nanofibrous Polymer Membranes for Water Treatment. *ACS Appl. Mater. Interfaces* **2014**, *6*, 14600−14607.
(16) Sun, F.; Li, X.; Xu, J.; Cao, P. Improving Hydrophilicity and Protein Antifouling of Electrospun Poly(vinylidenefluoride-hexafluoropropylene) Nanofiber Membranes. *Chin. J. Polym. Sci.* **2010**, *28*, 705−713.
(17) Mizrahi, B.; Khoo, X.; Chiang, H. H.; Sher, K. J.; Feldman, R. G.; Lee, J. J.; Irusta, S.; Kohane, D. S. Long-Lasting Antifouling Coating from Multi-Armed Polymer. *Langmuir* **2013**, *29*, 10087−10094.
(18) Wang, Y.; Chen, L. Electrospinning of Prolamin Proteins in Acetic Acid: The Effects of Protein Conformation and Aggregation in Solution. *Macromol. Mater. Eng.* **2012**, *297*, 902−913.
(19) Wang, Y.; Chen, L. Fabrication and Characterization of Novel Assembled Prolamin Protein Nanofabrics with Improved Stability, Mechanical Property and Release Profiles. *J. Mater. Chem.* **2012**, *22*, 21592−21601.
(20) Wang, Y.; Chen, L. Cellulose Nanowhiskers and Fiber Alignment Greatly Improve Mechanical Properties of Electrospun Prolamin Protein Fibers. *ACS Appl. Mater. Interfaces* **2014**, *6*, 1709−1718.
(21) Wang, C.; Tian, Z.; Chen, L.; Temelli, F.; Liu, H.; Wang, Y. Functionality of Barley Proteins Extracted and Fractionated by Alkaline and Alcohol Methods. *Cereal Chem.* **2010**, *87*, 597−606.
(22) Silva, S. S.; Maniglio, D.; Motta, A.; Mano, J. F.; Reis, R. L.; Migliaresi, C. Genipin-Modified Silk-Fibroin Nanometric Nets. *Macromol. Biosci.* **2008**, *8*, 766−774.
(23) Tian, H.; Wang, Y.; Zhang, L.; Quan, C.; Zhang, X. Improved Flexibility and Water Resistance of Soy Protein Thermoplastics Containing Waterborne Polyurethane. *Ind. Crops Prod.* **2010**, *32*, 13−20.
(24) Elazzouzi-Hafraoui, S.; Nishiyama, Y.; Putaux, J.; Heux, L.; Dubreuil, F.; Rochas, C. The Shape and Size Distribution of Crystalline Nanoparticles Prepared by Acid Hydrolysis of Native Cellulose. *Biomacromolecules* **2008**, *9*, 57−65.
(25) Kim, K.; Akada, Y.; Kai, W.; Kim, B.; Kim, I. Cells Attachment Property of PVA Hydrogel Nanofibers Incorporating Hyaluronic Acid for Tissue Engineering. *J. Biomater. Nanobiotechnol.* **2011**, *2*, 353−360.
(26) Tsuji, H.; Nakano, M.; Hashimoto, M.; Takashima, K.; Katsura, S.; Mizuno, A. Electrospinning of Poly(lactic acid) Stereocomplex Nanofibers. *Biomacromolecules* **2006**, *7*, 3316−3320.
(27) Xin, Y.; Huang, Z. H.; Yan, E. Y.; Zhang, W.; Zhao, Q. Controlling Poly(*p*-phenylene vinylene)/Poly(vinyl pyrrolidone) Composite Nanofibers in Different Morphologies by Electrospinning. *Appl. Phys. Lett.* **2006**, *89*, 053101/1−053101/3.
(28) Yang, C.; Wang, Y.; Vasanthan, T.; Chen, L. Impacts of pH and Heating Temperature on Formation Mechanisms and Properties of Thermally Induced Canola Protein Gels. *Food Hydrocolloids* **2014**, *40*, 225−236.
(29) Sun, B.; Long, Y.; Liu, S.; Huang, Y.; Ma, J.; Zhang, H.; Shen, G.; Xu, S. Fabrication of Curled Conducting Polymer Microfibrous Arrays via a Novel Electrospinning Method for Stretchable Strain Sensors. *Nanoscale* **2013**, *5*, 7041−7045.
(30) Wu, H.; Hu, Q.; Zhang, L.; Fong, H.; Tian, M. Electrospun Composite Nanofibers of Polybutadiene Rubber Containing Uniformly Distributed Ag Nanoparticles. *Mater. Lett.* **2012**, *84*, 5−8.
(31) Xia, Y.; Wang, Y.; Chen, L. Molecular Structure, Physicochemical Characterization, and in Vitro Degradation of Barley Protein Films. *J. Agric. Food Chem.* **2011**, *59*, 13221−13229.
(32) Belazi, D.; Solé-Domènech, S.; Johansson, B.; Schalling, M.; Sjövall, P. Chemical Analysis of Osmium Tetroxide Staining in Adipose Tissue Using Imaging ToF-SIMS. *Histochem. Cell Biol.* **2009**, *132*, 105−115.
(33) Higuchi, T.; Tajima, A.; Motoyoshi, K.; Yabu, H.; Shimomura, M. Suprapolymer Structures from Nanostructured Polymer Particles. *Angew. Chem., Int. Ed.* **2009**, *48*, 5125−5128.
(34) Trindade, A. C.; Canejo, J. P.; Teixeira, P. I. C.; Patrício, P.; Godinho, M. H. First Curl, Then Wrinkle. *Macromol. Rapid Commun.* **2013**, *34*, 1618−1622.
(35) Luchnikov, V.; Ionov, L.; Stamm, M. Self-Rolled Polymer Tubes: Novel Tools for Microfluidics, Microbiology, and Drug-Delivery Systems. *Macromol. Rapid Commun.* **2011**, *32*, 1943−1952.
(36) Kim, S.; Xu, J. Aggregate Formation of Zein and Its Structural Inversion in Aqueous Ethanol. *J. Cereal Sci.* **2008**, *47*, 1−5.
(37) Berim, G.; Ruckenstein, E. Contact Angle of a Nanodrop on a Nanorough Solid Surface. *Nanoscale* **2015**, *7*, 3088−3099.
(38) Silveira, R. L.; Stoyanov, S. R.; Gusarov, S.; Skaf, M. S.; Kovalenko, A. Supramolecular Interactions in Secondary Plant Cell Walls: Effect of Lignin Chemical Composition Revealed with the Molecular Theory of Solvation. *J. Phys. Chem. Lett.* **2015**, *6*, 206−211.
(39) Anderson, J. M. Biological Responses to Materials. *Annu. Rev. Mater. Res.* **2001**, *31*, 81−110.
(40) Ji, F.; Lin, W.; Wang, Z.; Wang, L.; Zhang, J.; Ma, G.; Chen, S. Development of Nonstick and Drug-Loaded Wound Dressing Based on the Hydrolytic Hydrophobic Poly(carboxybetaine) Ester Analogue. *ACS Appl. Mater. Interfaces* **2013**, *5*, 10489−10494.
(41) Jhong, J. F.; Venault, A.; Liu, L.; Zheng, J.; Chen, S.; Higuchi, A.; Huang, J.; Chang, Y. Introducing Mixed-Charge Copolymers As Wound Dressing Biomaterials. *ACS Appl. Mater. Interfaces* **2014**, *6*, 9858−9870.
(42) Chen, L.; Remondetto, G.; Rouabhia, M.; Subirade, M. Kinetics of the Breakdown of Cross-linked Soy Protein Films for Drug Delivery. *Biomaterials* **2008**, *29*, 3750−3756.
(43) Pandey, H.; Parashar, V.; Parashar, R.; Prakash, R.; Ramteke, P. W.; Pandey, A. C. Controlled Drug Release Characteristics and Enhanced Antibacterial Effect of Graphene Nanosheets Containing Gentamicin Sulfate. *Nanoscale* **2011**, *3*, 4104−4108.

DOI: 10.1021/acsami.5b02129
ACS Appl. Mater. Interfaces 2015, 7, 13422−13430